JACS
JOURNAL OF THE AMERICAN CHEMICAL SOCIETY
Article
pubs.acs.org/JACS

Size Effect and Odd−Even Alternation in the Melting of Single and Stacked AgSC*n* Layers: Synthesis and Nanocalorimetry Measurements

Lito P. de la Rama,[†] Liang Hu,[†,§] Zichao Ye,[†] Mikhail Y. Efremov,[‡] and Leslie H. Allen*[,†]

[†]Department of Materials Science and Engineering and Coordinated Science Laboratory, University of Illinois at Urbana—Champaign, Urbana, Illinois 61801, United States

[‡]Department of Chemical and Biological Engineering and Center for Nanotechnology, University of Wisconsin—Madison, Madison, Wisconsin 53706, United States

Supporting Information

ABSTRACT: We report a systematic study of melting of layered lamella of silver alkanethiolates (AgSC*n*). A new synthesis method allows us to independently change the thickness of the crystal in two ways—by modulating chain length (n = 7−18) and by stacking these crystals to a specific layer number (m = 1−10). This method produces magic size lamella, having a well-spaced discrete melting point, T_m, distribution. Nanocalorimetry shows stepwise increases in T_m, as the lamella thickness increases by integer increments of chain length. The relationship between T_m and the inverse thickness follows the linear scaling law of Gibbs−Thomson effect. Layer stacking dramatically changes the degree and nature of size-effect melting. There is odd/even effect in stacked 2, 3, and 4 layers. T_m values of single-layer and multilayer samples do not show noticeable odd/even alternation. We develop a phenomenological model of size effect based on the cumulative excess free energy, G_{excess}, contributions of four spatially separate regions of the crystal: surface, Ag−S central plane, substrate interface, and interlayer interface. The selective appearance of the odd/even effect is due to the significant stabilization (1.4 kJ/mol) of interlamellae interfaces of odd-chain samples, possibly due to registration/packing. Stabilization occurs only for the mobile lamellae situated close to the free surface, and thus 2-layer samples show the highest degree of stabilization. X-ray diffraction shows that the chains are tilted 18° with respect to the basal plane normal but that the van der Waals gap is 0.3 Å smaller for crystals with odd chains.

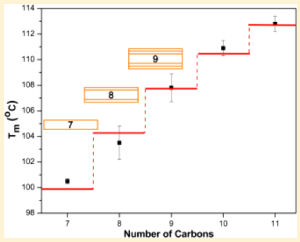

1. INTRODUCTION

Self-assembly for nanoscale systems is important in the continuing push toward miniaturization. Understanding the thermodynamic properties at the nanoscale is critical in the self-assembly process. Size-dependent phenomena dominate at these small sizes, such as the observation of size-dependent melting point (T_m).[1−4] Values of T_m can decrease by hundreds of degrees from bulk values as the size decreases to the nanometer scale. For small sizes, the effect of the surface plays a key role in changing the overall thermodynamic properties of the system. In addition, both electronic[5] and the shape[6] characteristics of nanometer size clusters and adhesion properties of thin films[7] can be dramatically altered by designing specific surface properties.

The term "magic number sizes" was first coined to describe the anomalous stability of certain isotopes containing a specific number of neutrons.[8,9] On the molecular level, magic sizes were discovered in vapor cluster beams of noble gases and metals.[10−14] Recently, magic sizes have also been observed in our group in indium clusters on surfaces[15] and in organic monolayer-protected clusters with a 102 atom Au core.[16] During synthesis of these systems, certain sizes dominate more than others by being more stable. This changes the size distribution from continuous to discrete. Melting points of these particles also exhibit discrete behavior, as shown for example in Figure 1a for indium clusters.[15] The inset shows the in situ nanocalorimetry measurement during indium deposition. The periodic multiple peaks in the calorimetry results show unique melting points for magic sizes of indium clusters formed during deposition. These magic sizes correspond to the formation of clusters with the addition of complete atomic shells (geometric magic number) as shown in the diagram. Size-dependent melting point for these clusters is clearly observed in the stepwise increase in the melting temperature corresponding to the discrete change in the cluster size. Not all materials (cluster) exhibit magic size formation (e.g., Sn, Bi).[17,18]

In 2D systems (lamella), magic size is applicable because the synthesis method naturally produces individual crystals with specific integer (1, 2, 3...) unit thickness. We achieve this discrete thickness change by incremental addition of one CH_2 group to the alkanethiol chain length and the discrete layer-by-layer addition to the growing lamella stack.

Nanocalorimetry (NanoDSC),[19−22] developed in our group, is the key thermal analysis tool used in this study. Thermodynamic measurements at the nanoscale require this special instrumentation technique due to the high sensitivity needed to measure the small signals from nanoscale materials.

Received: June 14, 2013
Published: August 26, 2013

   dx.doi.org/10.1021/ja4059958 | J. Am. Chem. Soc. 2013, 135, 14286−14298

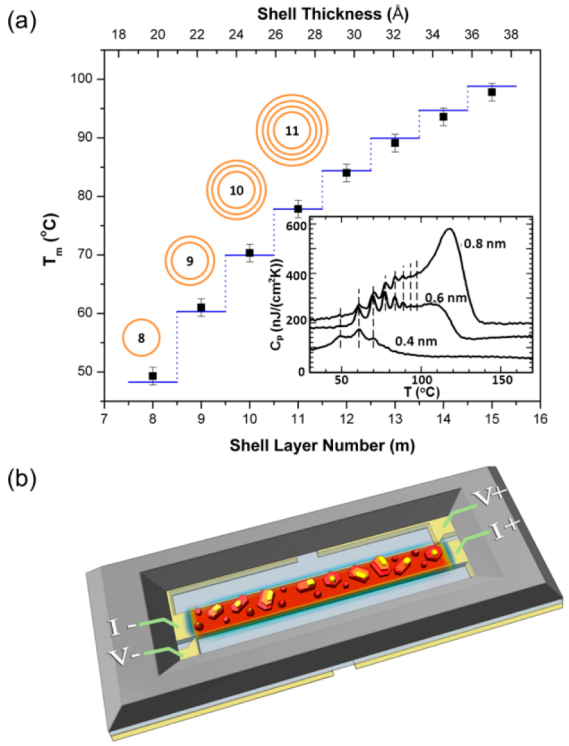

Figure 1. (a) Magic number size melting for indium clusters from in situ nanocalorimetry measurement during deposition. Inset shows periodic multiple peaks corresponding to the different magic size clusters. (b) Schematic of the nanocalorimetry sensor.[27]

NanoDSC is a chip-based calorimetry device fabricated on a silicon wafer. A SiN membrane patterned with a metal thin film constitutes the low thermal mass calorimetric cell shown in Figure 1b. It has been successfully used in the study of the size-dependent melting of metal nanoparticles,[15,23,24] polymer thin films,[25] and self-assembled monolayers.[26]

Silver alkanethiolate (AgSC*n*) is a layered lamellar compound which is a product of the self-assembly reaction between silver and alkanethiols. Dance et al.[28] first reported the synthesis and characterization of AgSC*n* from the precipitates of the reaction between silver salts and alkanethiols in solution. AgSC*n* is composed of a central plane of Ag and S with fully extended alkyl chains on both sides forming a bilayer ribbon-like structure.[28−33]

Currently, lamella is of interest in a variety of technological and scientific fields. For example, single- and multilayer lamella serve as platforms for organic monolayer electronics and lithography.[34,35] In biological studies, lamella acts as a model system for cell membranes, which are composed of single-layer phospholipid bilayer lamella.

In prior works, our group has successfully grown multilayer[27] and single-layer[36] AgSC*n* on different substrates using a vapor synthesis method. This method allows for systematic control of the number of layers in the final product.

In this paper, we combine the unique capabilities of the nanocalorimetry technique with the controlled synthesis method of AgSC*n* allowing for a systematic, fundamental thermodynamic study of the melting behavior of layered lamella. Discrete changes in the thickness of AgSC*n*, analogous to discrete "magic" size distribution, are achieved by changing the chain length of the alkanethiol and controlling the number of layers in the lamella. We show size-effect melting as a function of the lamella thickness. We also show a large odd/even effect in T_m for stacked AgSC*n* crystals with 2, 3, and 4 layers which is not present in single layers and multilayers (>10 layers). Odd/even effect in the thickness measurement from X-ray diffraction is also discovered. A phenomenological model for size-effect melting in layered lamella is proposed based on contributions to the melting point from the surface, central plane, substrate interface, and interlayer interface segments.

2. EXPERIMENTAL SECTION

2.1. AgSC*n* Synthesis. *Materials:* Pure silver evaporation sources (99.99%) are pellets obtained from Kurt J. Lesker Company. Alkanethiols ($C_nH_{2n+1}SH$) with different chain lengths (n = 7−18) with purity of more than 95% are obtained from Sigma-Aldrich and used without further purification. Different substrates are used for the growth of AgSC*n* including single-crystal ⟨100⟩ silicon with just the

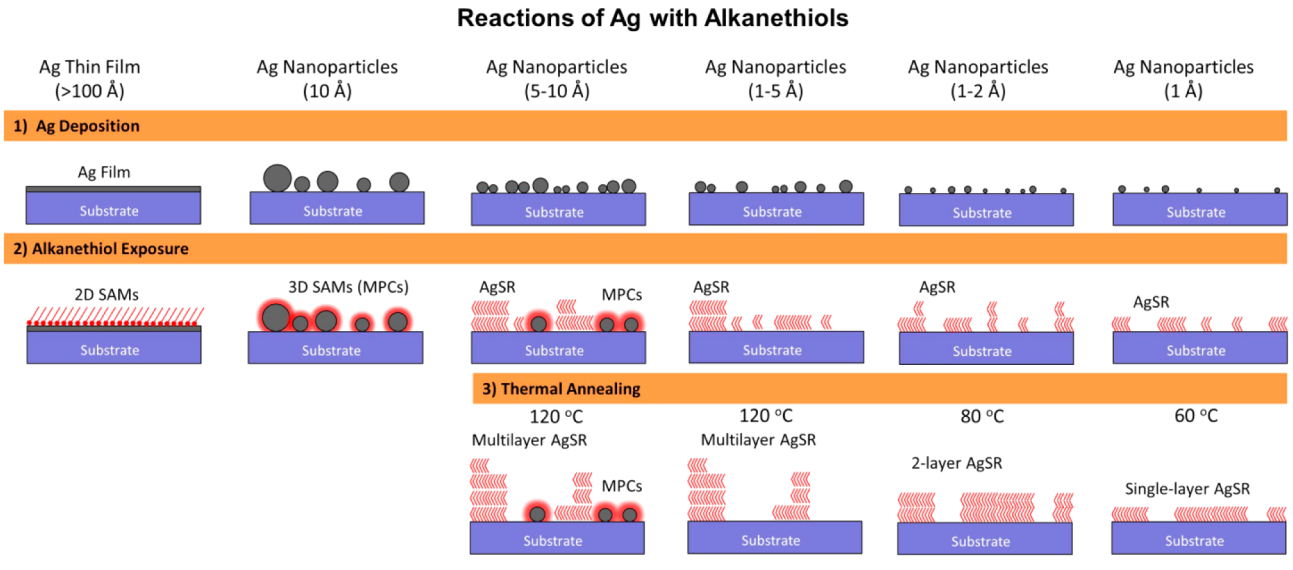

Figure 2. Schematic of the different reactions between Ag and alkanethiols. Controlled synthesis of AgSC*n* is achieved by varying the amount of Ag and the annealing temperature.[27,36]

dx.doi.org/10.1021/ja4059958 | J. Am. Chem. Soc. 2013, 135, 14286−14298

native oxide, single-crystal sapphire, and silicon wafers with low residual stress silicon nitride film.

Synthesis: The new vapor phase synthesis of AgSC*n* on different substrates has been reported in our prior publications for both the multilayer[27] and single-layer[36] samples. Figure 2 summarizes the overall synthesis process of different reactions between Ag and alkanethiols.[27,36] The amount of silver and the annealing temperature are two independent parameters to control the final synthesis product. This method offers an unprecedented control of the number of layers in AgSC*n* lamella, which allows for the systematic characterization of the thermodynamic properties as a function of the number of layers. Silver is deposited on different substrates via thermal evaporation at a base pressure of 5×10^{-8} Torr and a rate of 0.3 Å/s.

The amount of silver is determined using a quartz crystal monitor, and the deposition is controlled by a shutter coupled with a photodetector (solar cell) to determine the exact amount of time that the substrates are exposed to the source. The silver clusters on the substrates are then exposed to alkanethiol vapor for 3 days. The transfer time from the vacuum chamber is less than 30 min to ensure minimum contamination before the alkanethiol exposure. The substrates are then thermally annealed in vacuum (base pressure of 1×10^{-7} Torr), which minimizes the interaction of as-grown AgSC*n* with water and oxygen. Bensebaa et al.[30] reported that oxygen was not observed in AgSC*n* as deduced from their elemental analysis results. Furthermore, even though polar molecules (e.g., H_2O) have been attempted to be directly incorporated into AgSC*n* layers, none of these molecules were observed to be presented as deduced from XRD thickness measurements.[28] Multilayer crystals (>10 layers) are formed when the annealing temperature is greater than 100 °C for Ag amounts greater than 2 Å, whereas monodisperse single-layer crystals are formed for Ag amounts less than 1 Å and annealing temperature below 60 °C.

According to our prior work and the diagram in Figure 2, the small amount of silver used (1−5 Å) in this work is completely converted into AgSC*n* as the final product before annealing, as has been shown in the last three columns of Figure 2. In our previous publication,[27] we suggested that the growth of stacked multilayer AgSC*n* must involve long-range diffusion of AgSC*n* segments, both laterally (≈1000 nm) and vertically (10−100 nm) during annealing. Although at present the diffusing species active during annealing is unclear to us, the high rate of transport (>200 nm/h) on the substrate surface at such low annealing temperature (≤120 °C) implies that the diffusion species tend to be small.

2.2. Sample Characterization. *Nanocalorimetry:* This is a unique thermodynamic measurement platform developed in our group. The details of the design, fabrication, and operation of the nanocalorimetry device are discussed elsewhere.[19−21] In summary, the device is composed of a thin (100 nm) free-standing silicon nitride membrane supported at the periphery by a silicon substrate. On one side of the membrane is a patterned thin film metal (50 nm Pt or Al). The metal film and the silicon nitride membrane form the calorimetric cell with low thermal mass. AgSC*n* samples are directly grown on the silicon nitride surface on the opposite side of the metal heater. Sample alignment is achieved using a self-aligned shadow mask during silver deposition.[37] The metal film serves both as a heater via joule heating when current is applied and a thermometer after calibration to determine the temperature coefficient of resistance (TCR) of the film. Nanocalorimetry measurements are done in vacuum with a base pressure of 1×10^{-7} Torr. It is used in differential mode. Adiabatic conditions are achieved using fast heating rates (50 000 K/s) during the experiment. The experiments use only the first heating/cooling cycle since the fast heating and cooling rates used create noncrystalline products during the solidification from the melt. This is different than the slow heating and cooling rates of conventional DSC which shows good reversibility.[30−33] The plot of the heat capacity as a function of temperature, $C_p(T)$, is used to determine the melting temperature (peak location), enthalpy of melting (integrated area under the melting peak), and the amount of sample (shift in the C_p baseline above the melting point divided by the specific heat assumed to be the same as alkanes).

X-ray Diffraction: XRD measurements are done on a Philips X'pert diffractometer using Cu Kα radiation source with 1.5418 Å wavelength. The average lamellar thickness is determined from multiple reflections indexed as (0*k*0) with the lamella parallel to the substrate. Sample alignment is carried out via peak optimization of known crystal planes on the substrates, (004) for silicon and (006) for sapphire. The peak locations and average crystal size are determined using an automated peak fitting procedure via JADE X-ray analysis software.

Atomic Force Microscopy: The topography of the AgSC*n* crystals is studied using an Asylum MFP-3D AFM with sharp silicon nitride tips from Budget Sensors. We plot the height histograms to determine the number of layers in the AgSC*n* crystal. After an appropriate image flattening procedure to remove tilt in the sample during the scan, each height measurement for every pixel (one scan is 512 × 512 pixels) is plotted in a frequency distribution. The first peak corresponds to the lowest height in the image associated with the bare substrate surface after some corrections described in our prior publication.[36] Each subsequent peak corresponds to the surfaces of the AgSC*n* crystal with values in multiples of the thickness of 1 layer. These values are compared to the layer thickness measured using XRD.

3. RESULTS AND DISCUSSION

3.1. Single-Layer AgSC*n*: Nanocalorimetry. The T_m of single-layer AgSC*n* with increasing chain lengths is shown in Figure 3a. Our new synthesis method allows incremental change in chain length and directly controls by design the thickness of the lamella in discrete steps ($\Delta d \sim 2.4$ Å) with the addition of one methylene (CH_2) group to the chains on both sides. This has the effect of adding a complete planar "shell" to the 2D lamella. This is analogous to the magic number sized formation of indium clusters shown in Figure 1a. For indium, the discreteness in size ($\Delta d \sim 4.8$ Å) is due to the addition of one "complete shell" of atoms in the 3D cluster.

Nanocalorimetry measurements show large size-effect melting for single-layer AgSC*n*. Figure 3a shows the stepwise increase in T_m as a function of the chain length. The $C_p(T)$ plots for each chain length are shown in the inset. These plots show that T_m increases in discrete steps as the chain length is increased by integer units. The error bars represent the variation from multiple experiments with each peak showing the average T_m. Each sample used for this figure consists of lamella with only 1-layer thickness as verified with AFM measurements.

This result is analogous to the discrete T_m in indium 3D spherical particles shown in Figure 1a.[15] The results show that size-effect melting is observed in both 3D nanoparticles and 2D lamellar sheets. For both indium and AgSC*n*, the addition of a complete shell/layer of atoms to the growing structure, either in spherical or lamellar form, results in a discrete increase in T_m. It is noteworthy that these systems by themselves may be thought of as completely different (3D vs 2D; metal vs organic), yet the same phenomenon of T_m depression is observed. The underlying thermodynamic principle that gives rise to this phenomenon is the same for both systems.

Models of size-dependent melting relate T_m with the size (d) of the object. The qualitative explanation for this phenomenon is that atoms/molecules at or near the surface are different (bonding, organization, steric limitation, etc.) as compared to the inner bulk-like atoms/molecules. As a consequence, the normalized free energy of the total system (J/cm^3) which includes the inner as well as the surface region atoms will be slightly different than that of bulk material and thus will melt at a slightly higher or lower temperature. This excess free energy, ΔG_{excess} (J/cm^2), is due to the surface region and scales with

dx.doi.org/10.1021/ja4059958 | J. Am. Chem. Soc. 2013, 135, 14286−14298

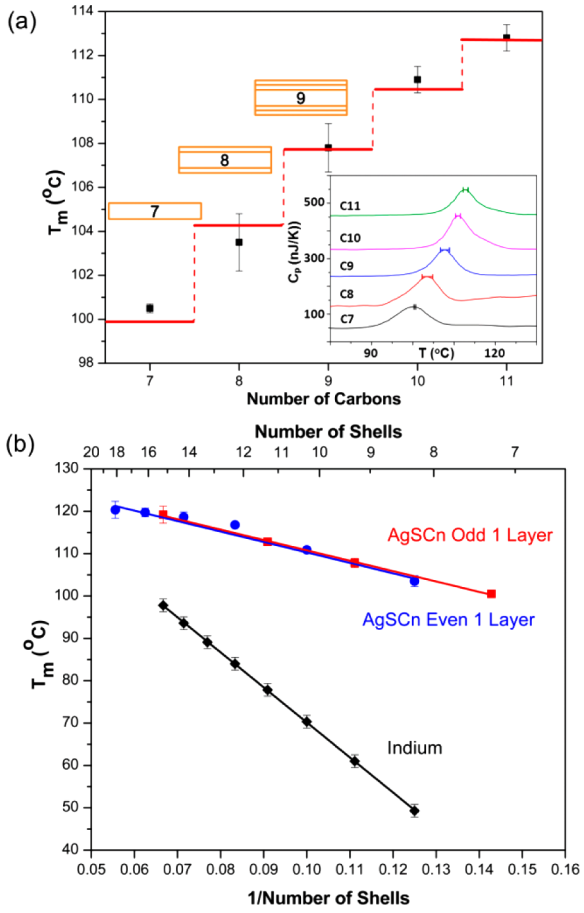

Figure 3. (a) Size-effect melting for single-layer AgSC*n* with different chain lengths showing a stepwise increase in T_m analogous to the magic size melting of indium clusters. The temperature steps are calculated from the linear fit in (b). Inset shows the $C_p(T)$ plots for different chain lengths with the T_m peaks representing the average of multiple experiments. Plots are offset vertically for clarity. (b) Inverse linear relationship between T_m and $1/d$ for AgSC*n* and indium.

particle surface area. Therefore, the deviation of ΔT_m scales with $1/d$ and can be expressed as the following equation:

$$T_m = T_m^o\left(1 - \frac{G_{excess}}{H_m^o d}\right) \rightarrow T_m = T_m^o\left(1 - \frac{2\sigma}{H_m^o d}\right) \quad (1)$$

Melting of indium $T_m(1/d)$ as shown in Figure 3b is a typical result for a variety of metals such as Au and Sn.[3,23,38] This relationship can be quantitatively described using the classical Gibbs−Thomson (G−T) theory[39] in eq 1. In the G−T model, the excess free energy term in the numerator is directly related to surface energy of the particle.

For 3D metallic clusters, this relationship is best represented by Pawlow's variation of the G−T model which quantifies this G_{excess} as the change in the surface energies (normalized for atomic density) from the solid to the liquid state upon melting.[40] For 2D aliphatic lamellar systems, the same relationship can be derived as previously shown for polyethylene, where size-effect melting has been extensively studied and shown to be dependent on the thickness of the lamella.[41,42] This relationship is quantified in the model proposed by Lauritzen, Hoffman, and Weeks (LHW)[43−45] with the resulting linear relationship similar to that of the G−T equation. The excess free energy in the LHW model is related to an "interfacial surface energy" due to the fold region of the polyethylene chain at the interface.

The plots of T_m versus $1/d$, represented as the number of carbons in the chain for AgSC*n* and the number of shells for indium, are shown in Figure 3b. Both indium and 1-layer AgSC*n* show an inverse linear relationship. The discrete steps in Figures 1a and 3a represent the calculated values of the melting point from the linear fit in Figure 3b. The slope of the line gives a value for the excess free energy, G_{excess}, and will be discussed later in the modeling section.

The study of the melting of single-layer lamella, to our knowledge, has not been previously reported, and thus our results cannot be easily compared to other aliphatic lamellar systems. The most analogous structure to our single-layer lamella is the self-assembled monolayer of alkanethiol on metal substrates (Au or Ag) which contains a terminal methyl group at one end and a thiol group bonded to a metal in the other.[46−48] However, the melting transition of SAMs is not well-defined. Results from XRD[49] and nanocalorimetry[26] measurements show a broad phase transition range between ∼70 and 125 °C (fwhm ∼ 50 °C). AgSC*n*, on the other hand, has a very sharp transition (fwhm ∼ 7 °C).

Despite obvious differences, comparison of our single-layer AgSC*n* results with that of multilayer alkane lamella remains instructive. Both structures contain fully extended alkyl chains, and the majority of the energetics or enthalpy of melting transition (∼4 kJ/mol(CH_2)) for both systems is attributed to the inner $-CH_2-$ nearest neighbor chain-to-chain van der Waals interaction. Here we note two important differences between 1-layer AgSC*n* and *n*-alkanes of similar size: (1) T_m of 1-layer AgSC*n* is much higher than alkanes (bulk multilayer) of the same chain length and (2) the odd/even effect on the T_m of 1-layer AgSC*n* is absent.

The first difference is the high melting point of AgSC*n* compared to that of alkanes of comparable chain lengths. An example is that of 1-layer AgSC7 which melts at T_m = 100 °C and is much higher than those of C_7H_{16} ($T_m \approx -90$ °C) or $C_{14}H_{30}$ ($T_m \approx 5$ °C), which are the equivalent 1/2 bilayer and full bilayer thickness, respectively. We attribute this difference to the contribution made to ΔG_{excess} from the tightly bound −S−Ag− central plane. This produces a positive change in the overall free energy as compared to the negative value due to the surface region. The positive change will be discussed in detail in the later section of the paper after the effects of stacking are addressed. This effect of higher values of T_m (vs alkane) is also present in self-assembled monolayers (SAMs) of AuSCn where T_m ∼ 100 °C has been reported.[26,49] For SAMs, one end of the alkyl chain is also covalently bound to a metal atom in the Au−S network so the effects are similar to that of the Ag−S central plane in AgSC*n*.

The second difference concerns the odd−even alternation of T_m which is well-documented for *n*-alkanes: even-numbered alkanes melt at higher temperatures than odd-numbered alkanes. For example, C_8H_{18} (T_m = −57 °C) melts at ΔT_m ∼ 15 °C above the extrapolated values based on C_7H_{16} (T_m = −90 °C) and C_9H_{20} (T_m = −54 °C). However, in our case, the odd/even effect is not present in single-layer AgSC*n*. The T_m of AgSC8 extrapolated from that of AgSC7 and AgSC9 is approximately the same temperature (±1 °C) as the measured value. The linear fit in Figure 3b separated between the odd and even chains shows no significant difference for single-layer AgSC*n*.

dx.doi.org/10.1021/ja4059958 | J. Am. Chem. Soc. 2013, 135, 14286−14298

The absence of an odd/even effect is just as revealing as the presence. They both reveal the intrinsic nature of the material. Comparison of the odd/even effect for single-layer lamella is difficult to find. There is no experimental evidence of this effect for SAMs, although simulation studies have shown that there may be an odd/even variation.[50] However, there is a strong odd/even variation in the contact angle surface energy measurement in SAMs.[51] The relationship between surface energy and melting point is unclear, and they may be independent of each other. Surface energy may not be a good indicator of whether a corresponding odd/even variation in T_m will be present.

The nature of the terminal methyl group is a key factor in determining surface energy and melting properties of single-layer lamellae. For AgSC*n*, the terminal CH_3 group in both odd and even chains forms the free surface of the single-layer lamella and interacts via van der Waal's forces with the nearest neighbor CH_3 groups in adjacent chains. The end group orientations between odd and even chains are different relative to the central plane since the alkyl chain is tilted, as shown in Figure 4a. This has been found in simulation studies of an analogous structure using self-assembled monolayers (SAMs).[51,52] For alkanes, the orientation of the terminal CH_3 has no odd/even difference since the chains are not tilted. Measurements of the surface energy for alkanes also do not show the odd/even effect.[53] For AgSC*n*, we would expect alternating odd/even effect of surface energy.

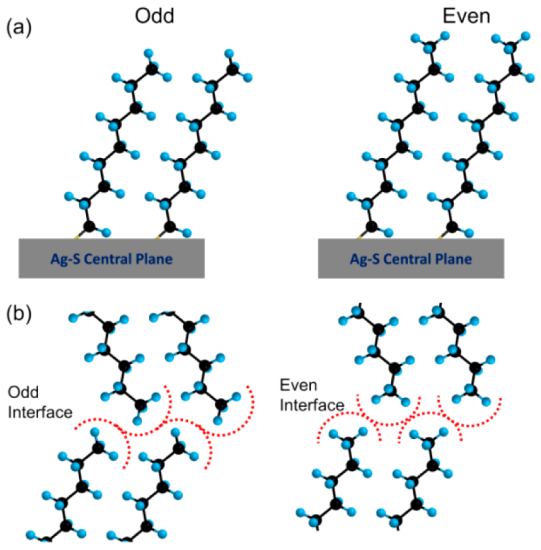

Figure 4. (a) Difference in the orientation of the terminal CH_3 group for both odd and even chains. This difference is due to the tilt of the alkyl chain relative to the central plane normal. (b) Different terminal CH_3 orientation affects the interface formed between layers for odd and even chains. As is shown, little interdigitation, if any, occurs ($\leq$0.9 Å), as deduced from our previous XRR and XRD results.[36]

Why is there no odd/even effect in the melting points of single layer AgSC*n*? The difference in orientation of the terminal methyl group relative to the surface does not change the closest neighbor distance, interaction, or local orientation when comparing odd or even chains. Thus the van der Waal's interaction between odd and even chains is invariant. The G_{excess} contributions from surfaces of the odd and even chains will not be significantly different, as will be shown in later sections, and which is consistent with the lack of an odd/even effect for single-layer AgSC*n*.

It is noteworthy that melting point measurements for lamellar alkane crystals are all done on multilayer samples, and the odd/even effect has been observed. To our knowledge, there is no measurement of T_m done on a purely single-layer alkane lamella having only free surface boundaries, but we speculate that there may be no odd/even effect in T_m for these crystals. Reports of "monolayer" alkanes on graphite are actually layers of alkanes that are oriented parallel to the substrate and still contain the end-to-end methyl group stacking.[54,55] The difference in the orientation of the terminal CH_3 plays a huge role in the close-packing structure when 2 layers are stacked where the terminal methyl groups from the 2 layers are mated to each other in forming the interface.[56,57] We see a large odd/even effect for stacked AgSC*n* as is observed in stacked alkanes. This highlights the importance of stacking and will be discussed in the succeeding sections.

3.2. Effect of Stacking: Melting of 2-Layer AgSC*n*. In the previous section, the thickness of AgSC*n* was increased by using successively longer chain lengths. However, by using our new vapor synthesis method, we can also increase the thickness of the crystal by the stacking process where any numbers (m) of single-layer lamella are stacked vertically. This allows us to grow crystals with as few as 2 layers. These 2-layer lamellae are naturally special crystals since they represent the most basic unit in the study of the effects of stacking—they contain only one interface.

The AFM images and the corresponding height histograms in Figure 5a,b show the change in the crystal thickness via stacking. Our controlled synthesis method has successfully grown both monodisperse crystals (1-layer and 2-layer samples) and a mixed crystal (both 1-layer and 2-layer in the same sample). Is there a difference in the outcome (T_m) between these two different means of increasing the thickness (d)? Yes, in both degree and character.

We find that the effect of stacking single layers of AgSC*n* on T_m is huge. Nanocalorimetry results in Figure 5c show a large increase in T_m between 1-layer and 2-layer (ΔT = 23 K for AgSC7) for a single-chain-length AgSC*n*. The same result is observed for other chain lengths.

This large increase in T_m upon stacking is somewhat surprising and is in contrast to PE crystals which show no significant effect of stacking. Figure 6 shows the plot of T_m versus $1/d$ for PE consisting of hundreds of stacked lamella layers where "d" is the thickness of the individual lamella from data reported in the literature.[42,59] Also shown in the figure is the one and only known data point for a 1-layer PE crystal (d = 12.5 nm) which was obtained using nanocalorimetry in our earlier work.[58] In contrast to AgSC*n*, the T_m of this single-layer sample is approximately the same as that of the stacked multilayer crystals with individual layer thickness that is also 12.5 nm but with a total thickness of several micrometers. Both samples melt at the same temperature, which is ~20 °C below the "bulk" value.

We deduce that changes produced by mating two 1-layer AgSC*n* crystals alter the energetics, rearrangement, and/or the mobility of the terminal methyl groups in the "contact" region. This changes the effective collective melting properties (e.g., G_{excess}) for the whole crystal. For PE, stacking has little effect on forming an "interface" and each 1-layer crystal acts independently and melts at the same T_m with or without being mated to each other.

dx.doi.org/10.1021/ja4059958 | J. Am. Chem. Soc. 2013, 135, 14286−14298

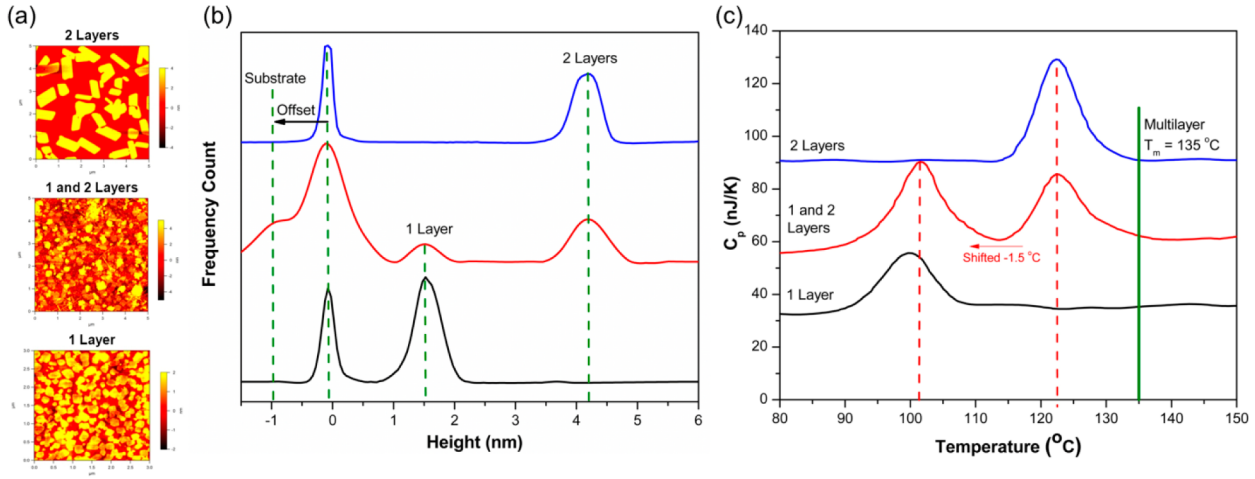

Figure 5. (a) AFM images of a monodisperse 1- and 2-layer AgSC7 and a mixture of both. (b) Corresponding height histograms showing the discrete changes in height when stacking layers. (c) Nanocalorimetry results showing a large increase in ΔT_m between 1 and 2 layers. The mixed sample (1-layer and 2-layer) shows two independent peaks which match those of the monodispered samples after a baseline correction $\Delta T = -1.5$ °C. This value of correction is within experimental error of the measurement due to the statistical variations arising from sample-to-sample calibration errors in the temperature parameter (±1.5 °C). The data for the mixed layer in the figure are the result of a single sample, whereas the data for the 1-layer and 2-layer monodispered are an average of five samples each.

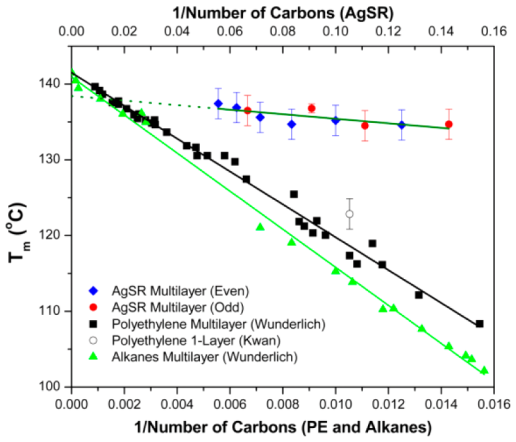

Figure 6. Plots of T_m vs $1/n$ for polyethylene (PE) and alkanes from reported data.[42,53] The single-layer PE data are from nanocalorimetry measurement done in our group.[58] The plot also contains the multilayer AgSC*n* results, which show minimal size-dependent melting behavior in contrast to PE and alkanes.

A closer look at the $C_p(T)$ data in Figure 5c shows that the values of the full width at half-maximum (fwhm) of the melting peaks of the 1-layer and 2-layer samples are the same (~7 °C) and yet the T_m has increased by $\Delta T \sim 23$ K. This infers that there exists a large degree of collective melting for each crystal and that the 2 crystal layers are strongly dependent and synergistic with each other. Together, the stacked layers have a much higher T_m than each individual crystal. We also note that the values of T_m for 1-layer and 2-layer in the mixed sample are the same as the monodisperse samples even though each sample is processed slightly differently having a different annealing temperature and amount of Ag. This attests to the invariability of the outcome with regards to the different processing conditions.

3.3. Effect of Stacking: Odd/Even Effect on 2-Layer AgSC*n*. The introduction of an interface not only increases the T_m for a 2-layer sample but also shows significant odd/even chain melting point alternation. By mating two, 1-layer crystals, the character of the crystal is changed such that it "knows" whether the chain length is odd or even. This is not true for 1-layer unstacked crystals where there is no odd/even effect.

Figure 7 shows size-effect melting for 2-layer AgSC*n* as a function of chain length. Observe the large oscillating odd/even difference with the T_m of the odd chains higher than the even chains. The odd/even effect persists for 3-layer and 4-layer samples. These plots include limited data due to the difficulty in resolving the small temperature differences for large values of n and m. The temperature steps in each plot are calculated from the linear fit of plots of T_m versus $1/n$ for each number of layers.

When separating the data into groups (odd and even chains), each individual group follows the size-effect inverse linear relationship as shown in Figure 8. In the 2-layer case, a large variation of $\Delta T \sim 12$ K is estimated due to the odd/even effect when extrapolating the value of the melting point of 2-layer AgSC7 from the linear fit of all even chains. In contrast, we find only an insignificant difference of $\Delta T \sim 1$ K when analyzing the 1-layer AgSC*n* in the same manner, and thus we conclude that the odd/even effect is absent in 1-layer AgSC*n*.

Why is there odd/even effect on the melting of stacked AgSC*n*? The odd/even effect in T_m has been a well-known phenomenon for *n*-alkanes for well over 100 years.[53,56] However, the explanation for the phenomenon remains unclear. It is typically attributed to differences in the "packing effects", interface density, and van der Waal's gap between odd and even alkanes.[56] Our data for AgSC*n* unambiguously show that the odd/even effect only occurs when layers are stacked, indicating a difference in the interlayer interaction of the terminal CH_3 groups between odd and even chains.

When stacking 2 layers, the difference in the orientation of the terminal CH_3 group in the odd and even chains has a significant role in the registration and the closest packing configuration.[52] For odd chains where the CH_3 groups are oriented away from the surface (tilted inward toward the central plane), the 2 layers can be packed closer, as shown in Figure 4b. The interlayer CH_3 distances are smaller compared to the even chains where the terminal CH_3 tilts away from the

dx.doi.org/10.1021/ja4059958 | J. Am. Chem. Soc. 2013, 135, 14286−14298

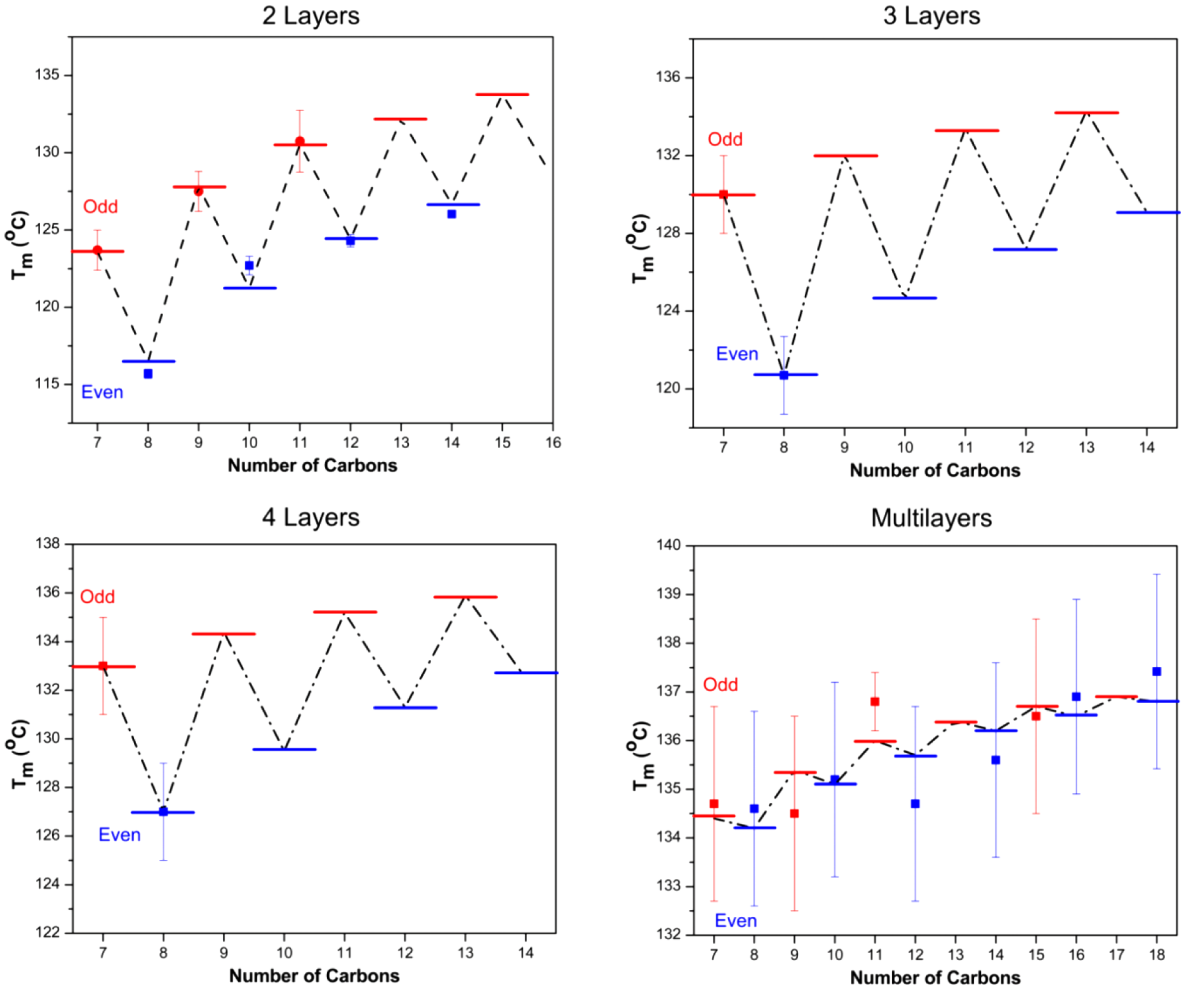

Figure 7. Odd/even alternation of T_m for 2-layer, 3-layer, 4-layer, and multilayer AgSC*n*. The temperature steps are calculated from the linear fit of T_m vs $1/n$ for each layer. For 3 and 4 layers, only data for AgSC7 and AgSC8 are determined, and the linear fitting assumes a T° calculated from the multilayer results.

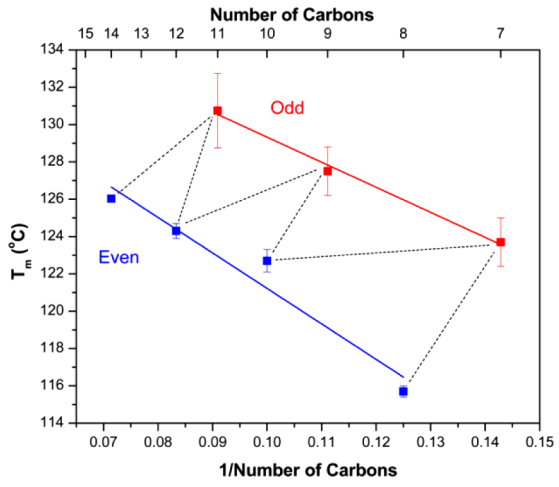

Figure 8. Inverse linear relationship between T_m and $1/n$ for 2-layer AgSC*n* separated between odd and even chains.

central plane and has a larger steric hindrance during interlayer packing. This is supported by XRD measurement of the lamella thickness, which also shows an odd/even effect and will be discussed in details later. The van der Waal's forces are different, thus the G_{excess} will also be different between odd and even chains. This leads to the large odd/even effect in T_m of stacked AgSC*n*.

3.4. Melting Point versus Number of Layers. The dependence of T_m to the number of layers in the lamellar stack opens a new level of discreteness in the size-effect melting of AgSC*n* lamella. A key feature of our new synthesis method allows us to grow crystals with 1, 2, 3, and 4 layers for AgSC7 and AgSC8. This level of discreteness is also analogous to the discrete sizes on magic sized materials. In this case, the change in thickness is in increments of a single lamella thickness. It becomes increasingly difficult to control the number of layers for longer chain lengths due to a limited annealing temperature range available. Multilayer crystals dominate the growth product at higher temperatures.

The T_m of AgSC7 and AgSC8 with different number of layers are shown in Figure 9a. There is a stepwise increase in T_m consistent with the discrete nature of the thickness change due to an increase in the number of layers. The plots for AgSC7 and AgSC8 highlight the odd/even effect which is also present in 3- and 4-layer samples. The multilayer samples included in the plots are for samples grown with at least 10 layers.

The temperature steps in Figure 9a are obtained from the calculated values of the melting point from the linear fit on the plot of T_m as a function of the inverse of the number of layers in Figure 9b. This linear behavior is consistent with the melting

dx.doi.org/10.1021/ja4059958 | J. Am. Chem. Soc. 2013, 135, 14286−14298

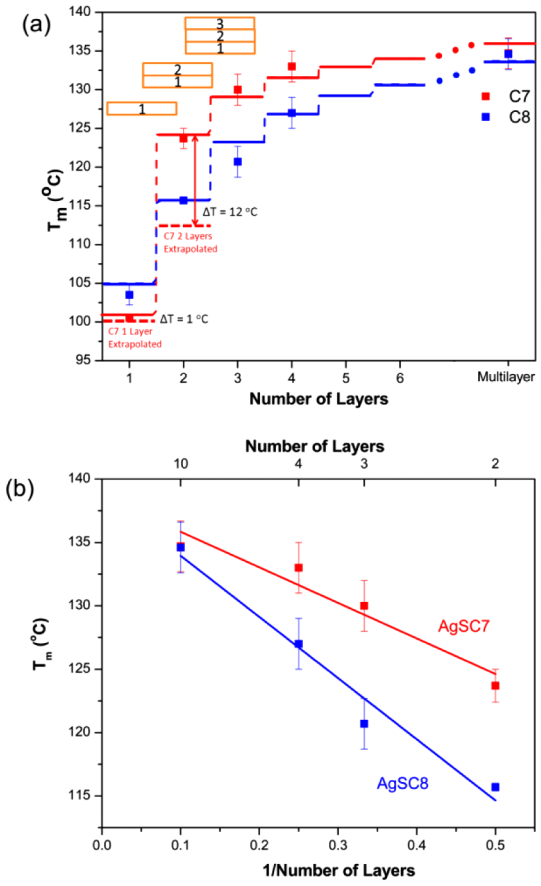

Figure 9. (a) T_m vs number of layers AgSC7 and AgSC8. The temperature steps are determined from the linear fit to the plot of T_m vs $1/m$. (b) Inverse linear plot for T_m vs $1/m$.

point depression described by the LHW model in eq 1. The thickness term for this case is represented by the number of bilayers multiplied by the chain length. Figure 9b plots T_m versus the inverse of the number of layers $(1/m)$ for the stacked samples. The single-layer results are not included in the linear fitting in order to separate the samples with contributions from the formation of an interface between layers when stacking is introduced.

3.5. Melting Enthalpy. The average measured value for H_m (enthalpy per mole of methylene group ΔH_{CH_2} = 3.85 ± 0.17 kJ/mol is an average value of our work and Levchenko et al. work[32]) for our multilayer AgSC*n* samples is the same as the reported[31−33] values for conventional DSC studies on bulk samples (ΔH_{CH_2} = 3.5−4.0 kJ/mol·CH_2). As expected, these values for AgSC*n* are consistent with values for alkanes and polyethylene (ΔH_m = 4.11 kJ/mol; ΔS_m = 9.9 kJ/mol·K).[42] However, values for H_m for single-layer AgSC*n* in this work are consistently (55%) lower than that for the multilayer samples. This systematic decrease in ΔH_m is expected, despite the large signal in the C_p data, due to the large uncertainty in determining the molar amount of Ag and AgSC*n* for single-layer samples. For 1-layer samples, only 0.5−1.0 Å of Ag is used for the reaction. Since our synthesis process is ex situ in nature and involves a 30 min exposure of Ag to ambient gases, there will be undoubtedly some undetermined amount of oxidation/sulfurization of Ag. For example, a 0.2 Å loss of Ag will result in a 50% decrease in our estimate for the molar amounts of AgSC*n*. Furthermore, the small amounts of alkanethiol residue[36] present on the SiN surface, which occurs during normal processing steps, will also lead to an addition underestimation for the value of AgSC*n* H_m. Thus the large uncertainty in the value in H_m for single-layer AgSC*n* is not surprising.

Interestingly, our analysis of the enthalpy data versus chain length *n* indicates that two of the methylene groups in the chain do not contribute to the overall enthalpy of the whole chain. This may also explain why AgSC2 has been found to be unstable in a previously reported work.[31] A complete study of enthalpy measurements of our AgSC*n* samples will be a subject of a future publication.

3.6. Phenomenological Model. The amount of size-effect depression in T_m in all material scales with the ratio of excess free energy (G_{excess}) to the size-corrected enthalpy ($H_m \times d$). For metal clusters, the models of Gibbs−Thomson and Pawlow relate G_{excess} to a single source—outer surface of the cluster. This can be tested independently by contact angle surface energy measurements of the liquid and solid. In the Lauritzen, Hoffmann, and Weeks model, the value of G_{excess} for planar stacked crystals of PE also has a single source—the folded region near the surface. In this case, however, the value of G_{excess} is 400% larger than contact angle surface energy measurements. G_{excess} includes the contributions not only from the surface but also from the whole fold region which is mostly buried and inaccessible to contact angle measurements.

The idea of using a single source/region to relate G_{excess} to ΔT is not consistent with our observations. No single expression can be generated incorporating values of thickness and G_{excess} that will yield our results. Our data of T_m versus $1/d$ do not fit a single line. This is highlighted by the observed odd/even effect in the stacked samples. For example, a 2-layer AgSC7 (d = 4.5 nm) melts at a higher temperature ($\Delta T \sim 8$ K) compared to a thicker 2-layer AgSC8 (d = 5.0 nm).

We propose to extend the form of these models for AgSC*n* and relate G_{excess} not to a single source but to four sources—four spatially segmented regions as shown in Figure 10a. In this way, we consider that the crystal melts collectively as a whole and occurs at a single temperature, T_m. However, this value of (size effect) T_m is determined by spatially separated regions of the crystal.

Changes in the molar enthalpy, entropy, and Gibbs energy of the *m*-layered AgSC*n* sample due to fusion are denoted as $\Delta H_{m,n}$, $\Delta S_{m,n}$, and $\Delta G_{m,n}$, respectively. The model is based on the representation of the above-mentioned thermodynamic values as sums of contributions of the methylene groups in the alkyl chains, free surface region, substrate−sample interface, interfaces between layers, and the central $-(Ag-S)_x-$ backbone. Corresponding indices of the values are CH2, S, Sub, I, and C, respectively. Then, for example, ΔH_{CH_2} is defined as the contribution of a mole of methylene groups. This model can be generalized for other lamellar crystals such as alkanes and polyethylene that do not have a central plane, by simply replacing the central plane with an interface. In fact, the AgSC*n* system can be thought of as an alkane lamellar crystal with an alternating end-to-end methyl interface and central plane Ag−S interface.

We follow Hohne's approach[60] to calculate the relationship between the melting point and the thickness of the lamella, which is an extension of the LHW model. In Hohne's approach, the thickness is represented with the number of carbons in the chain, and the excess energy parameter is defined as an excess

dx.doi.org/10.1021/ja4059958 | J. Am. Chem. Soc. 2013, 135, 14286−14298

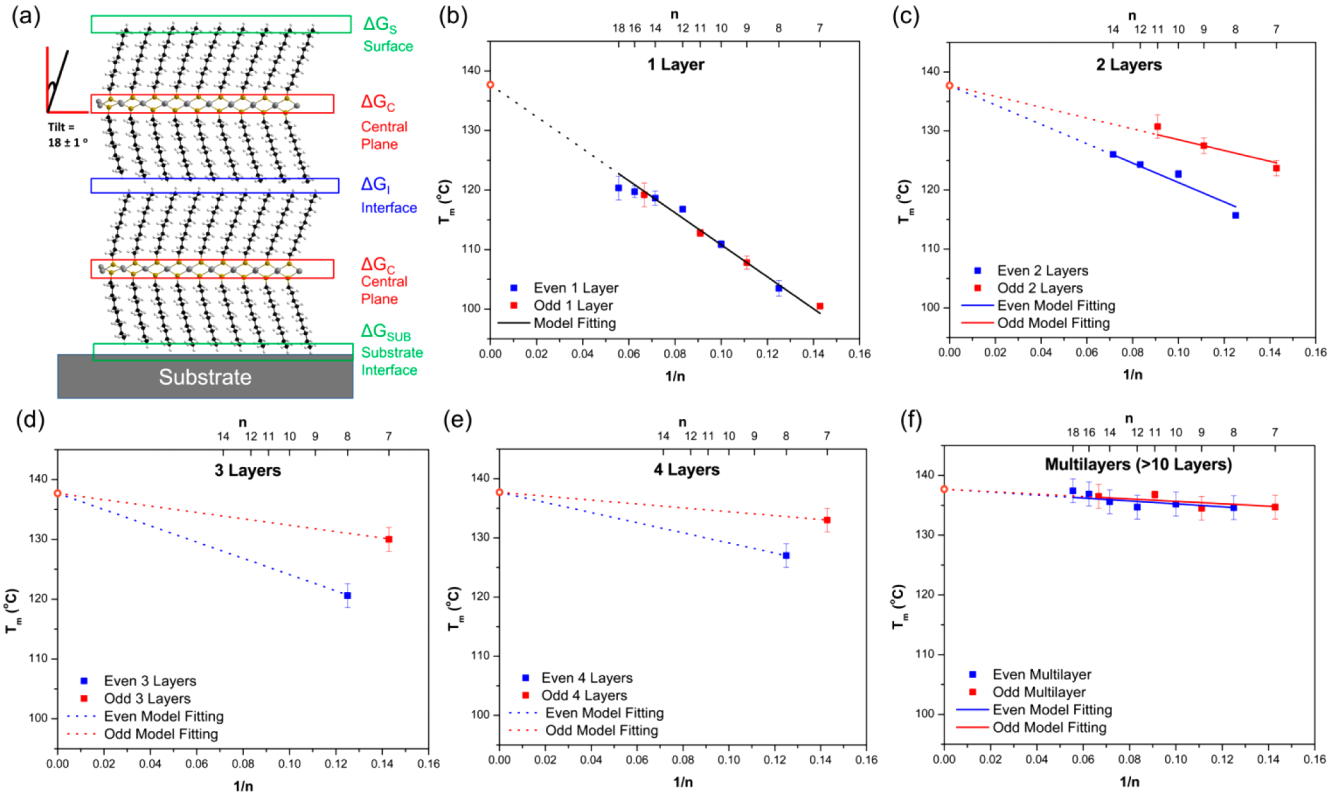

Figure 10. (a) Proposed model separating the excess energy contributions from the free surface, interlayer interface, central plane, and substrate interface regions. (b–f) Results of the model fitting procedure to the experimental data. This procedure fits all the experimental data simultaneously, instead of fitting different layers individually. The fitted value for T° = 137.7 °C is the same for all values m and included in all plots (b–f) as the orange circle at the y-intercept.

Gibb's free energy of the surface region. This surface region, however, can be more accurately characterized as an interface contribution since the data used for the model come from multilayer lamella of polyethylene and alkanes and not from single-layer samples. Nevertheless, Hohne's approach is instructive in our derivation.

For 1 mol of single-layer AgSCn, the molar enthalpy increments from the free surface, central backbone, and substrate interface regions are denoted as ΔH_S, ΔH_C, and ΔH_{SUB}, respectively. Molar enthalpy contribution from the interface between layers, ΔH_I, corresponds to the interface between two 1 mol single layers. Molar entropy contributions are defined in the same way. For the sake of brevity, only the key steps are included in the following quantitative analysis of the system. However, the complete mathematical analysis is given in the Supporting Information.

For 1 mol of single (m = 1) layer AgSCn, molar enthalpy can be expressed as

$$\Delta H_{1,n} = n\Delta H_{CH2} + \Delta H_S + \Delta H_C + \Delta H_{SUB} \quad (2)$$

Stacking m 1 mol single layers together, the expression for $\Delta H_{m,n}$ can be found

$$m\Delta H_{m,n} = mn\Delta H_{CH2} + \Delta H_S + m\Delta H_C + \Delta H_{SUB} + (m-1)\Delta H_I \quad (3)$$

Similarly, molar fusion entropy is expressed as

$$m\Delta S_{m,n} = mn\Delta S_{CH2} + \Delta S_S + m\Delta S_C + \Delta S_{SUB} + (m-1)\Delta S_I \quad (4)$$

At the transition temperature $T_{m,n}$ (K), the Gibbs energy $\Delta G_{m,n}$ equals 0:

$$\Delta G_{m,n}(T_{m,n}) = \Delta H_{m,n} - T_{m,n}\Delta S_{m,n} = 0 \quad (5)$$

Using eqs 3 and 4, eq 5 can be rewritten as

$$T_{m,n} = \frac{\Delta H_{m,n}}{\Delta S_{m,n}} = \frac{mn\Delta H_{CH2} + \Delta H_S + m\Delta H_C + \Delta H_{SUB} + (m-1)\Delta H_I}{mn\Delta S_{CH2} + \Delta S_S + m\Delta S_C + \Delta S_{SUB} + (m-1)\Delta S_I} \quad (6)$$

Limiting temperature T° is the asymptotic value of $T_{m,n}$ for $n \to \infty$:

$$T^{\circ} = \frac{\Delta H_{CH2}}{\Delta S_{CH2}} \quad (7)$$

For simplicity, we define the excess enthalpy and entropy as follows:

$$\Delta H_{excess} = \Delta H_S + m\Delta H_C + \Delta H_{SUB} + (m-1)\Delta H_I \quad (8)$$

$$\Delta S_{excess} = \Delta S_S + m\Delta S_C + \Delta S_{SUB} + (m-1)\Delta S_I \quad (9)$$

Algebraic simplification followed by a first-order Taylor expansion (for $1/n \to 0$) yields the relationship between $T_{m,n}$ and the thickness represented as the product of the number of carbons in the chain (n) and the number of layers (m) into the final Gibbs–Thomson form in eq 10. We define ΔG_I, ΔG_S, ΔG_{SUB}, and ΔG_C as the excess Gibb's free energy which are contributed from the interface, free surface, substrate interface,

dx.doi.org/10.1021/ja4059958 | J. Am. Chem. Soc. 2013, 135, 14286–14298

Table 1. Calculated Values of the Excess Free Energy Parameters

m	parameters	value	parameters	value
2	$\Delta G_C + \Delta G_I^{EVEN}$	-0.56 ± 0.13 (0.21)[a] kJ/mol	$\Delta G_C + \Delta G_I^{Odd}$	0.80 ± 0.12 (0.20)[a] kJ/mol
3		-0.65 ± 0.13 (0.21)[a] kJ/mol		0.51 ± 0.11 (0.20)[a] kJ/mol
4		-0.23 ± 0.12 (0.20)[a] kJ/mol		0.43 ± 0.10 (0.20)[a] kJ/mol
∞		-0.23 ± 0.09 (0.19)[a] kJ/mol		-0.19 ± 0.08 (0.18)[a] kJ/mol
all	T^o	137.7 ± 0.8 °C	$\Delta G_S + \Delta G_{SUB} + \Delta G_C$	-2.52 ± 0.08 (0.18)[a] kJ/mol

[a]The first value of uncertainty is obtained from the fitting procedure and assumes that the value of ΔH_{CH2} is fixed at 3.85 kJ/mol without error. The second value of uncertainty shown in parentheses (e.g., (0.21)[a]) is the total error including the uncertainty of $\Delta H_{CH2} = 3.85 \pm 0.16$ kJ/mol.

and central plane regions, respectively. For example, $\Delta G_I = \Delta H_I - T^o \Delta S_I$

$$T_{m,n} = T^o\left[1 + \frac{\Delta G_S}{mn\Delta H_{CH2}} + \frac{m\Delta G_C}{mn\Delta H_{CH2}} + \frac{\Delta G_{SUB}}{mn\Delta H_{CH2}} + \frac{(m-1)\Delta G_I}{mn\Delta H_{CH2}}\right] \quad (10)$$

The fitting procedure uses m and n as independent parameters and $T_{m,n}$ as the dependent one. Apparently, due to a strong dependency between fitting parameters, only certain combinations of them can be found. Consequently, eq 10 should be appropriately rewritten. By grouping m-dependent and m-independent parameters together, eq 10 can be transformed into a form more suitable for the fitting procedure.

$$T_{m,n} = T^o\left(1 + \frac{\Delta G_C + \Delta G_I}{n\Delta H_{CH2}} + \frac{\Delta G_S + \Delta G_{SUB} - \Delta G_I}{mn\Delta H_{CH2}}\right) \quad (11)$$

Here, we use $\Delta H_{CH2} = 3.85 \pm 0.17$ kJ/mol for our fitting.

However, the implicit assumption that the parameters of the fitting eq 11 are constant for all n and m has a fundamental problem. Constant parameters cannot explain the odd/even effect that appears at $m = 2$, $m = 3$, and $m = 4$ and apparently does not exist at $m = 1$ and $m \to \infty$ (multilayers). Let us hypothesize that the film surface, interface with the substrate, and $-(Ag-S)_x-$ central plane are the same for both odd and even AgSCn. Linear behavior of fusion temperature with n for single layer can be used as an argument that $(\Delta G_S + \Delta G_{SUB} + \Delta G_C)$ is constant at least for $m = 1$. For this analysis, this is assumed to be true for all m. Then the alternation of $T_{m,n}$ for $m = 2$, 3, and 4 can be represented as different free fusion energies ΔG_I^{Odd} and ΔG_I^{Even}, associated with odd and even chains, respectively. The difference vanishes for multilayers, which implies that ΔG_I also depends on m. It is also important that fusion temperatures, taken separately for both odd and even chains, lie well on the straight line segments, as shown in Figure 10b–f. It means that at least for $m = 2$ and for $m \to \infty$ (where the experimental data are present for different n) ΔG_I^{Odd} and ΔG_I^{Even} do not depend on n significantly. Taking all these considerations into account, the fitting procedure is modified to search for separate $\Delta G_{I,m}^{Odd}$ and $\Delta G_{I,m}^{Even}$ values ($m = 2$, 3, 4, and ∞) instead of the single ΔG_I parameter. The calculated parameters are given in Table 1.

The excess free energy for the lamellae interfaces ΔG_I has negative value since the interface is formed by weak forces in comparison with strong covalent bonds along the hydrocarbon chains. In opposite, the excess free energy associated with the central plane is expected to be positive. Then, the $(\Delta G_C + \Delta G_I)$ sum may have either sign. For even chains, negative ΔG_I is dominating. Small increase of ΔG_I^{Even} from 2 layers ($m = 2$) to multilayers ($m > 10$) can be observed in Figure 11a. The difference is about 0.4 kJ/mol.

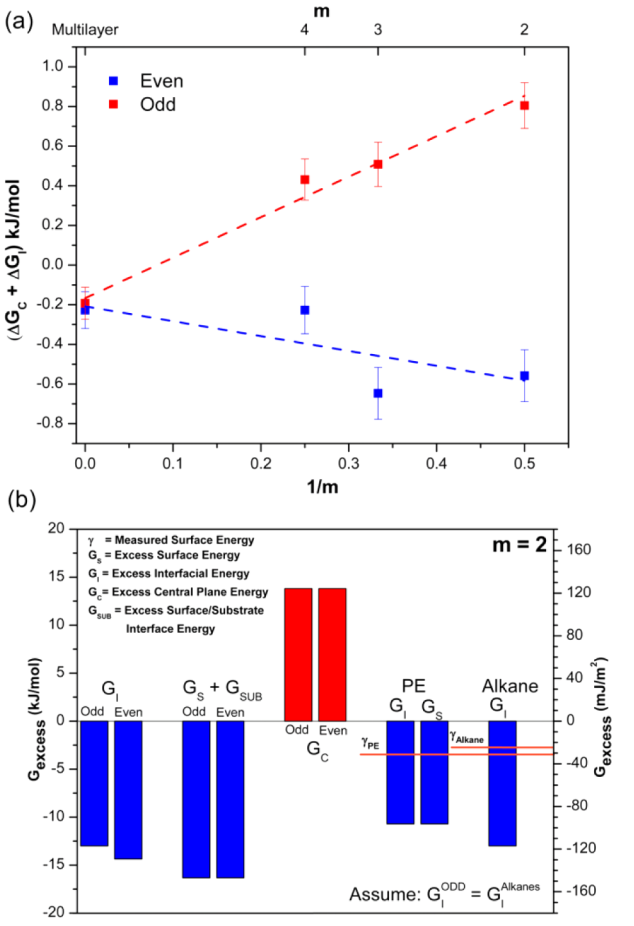

Figure 11. (a) Plot of the fitting results for $(\Delta G_C + \Delta G_I)$ for both odd and even chains. Significantly different behaviors are observed for odd and even chains which can be attributed to the stabilization of the interlamellae interfaces for odd chains. (b) Comparison of the excess free energies with PE and alkanes for $m = 2$. The G_S for alkanes is not known since no studies of purely single-layer samples are available.

However, the main intrigue in the fitting data is the significant stabilization of interlamellae interface for odd chains, which can be seen for 2, 3, and 4 layers, but fades completely in multilayers. The magnitude of the effect in 2 layers $(\Delta G_{I,m=2}^{Odd} - \Delta G_{I,m=2}^{Even})$ is about 1.3 kJ/mol.

It can be hypothesized that the top lamella (close to the free film surface) has enough mobility to adjust its position and form an optimal registration/packing with the adjacent lamella, thus stabilizing the interface. Lamellae far from the free surface in the multilayered samples do not have enough mobility under

dx.doi.org/10.1021/ja4059958 | J. Am. Chem. Soc. 2013, 135, 14286–14298

the annealing conditions, so that the value of $\Delta G_{I,m\to\infty}^{Odd}$ and $\Delta G_{I,m\to\infty}^{Even}$ are almost the same.

It may also be useful to relate these relative differences on an absolute basis for the purposes of comparing it with other materials. We can do this by assigning an absolute value to any one of the free energy parameters. In this case, we choose to assign the value of $\Delta G_I^{ODD} = -13.0$ kJ/mol, which is the same value as that for stacked alkanes and assume that $G_S = G_{SUB}$. The other excess free energy parameters are then calculated using the results of the model fitting. The values for all of the free energy parameters given on an absolute basis are shown in Figure 11b and compared to alkanes and polyethylene. The values of the surface and interfacial energies for polyethylene are assumed to be the same in order to be consistent with the experimental results that a single layer melts at the same temperature as the multilayer. For alkanes, only the value of the interfacial energy can be calculated from reported data on multilayer samples. These excess free energies differ greatly from the measured surface energy using contact angle measurements.

These findings that single-layer lamella does not show odd/even effect while stacked 2, 3, and 4 layers show significant odd/even effect are relevant to the thermodynamic study of layered aliphatic systems. The stabilization of the interface for odd chains may be a common cause for the odd/even effect in other systems. Controlling the number of layers in layered systems can be challenging, and systems that are mostly composed of single layers may not show an odd/even effect, but stacked samples will behave differently.

3.7. Odd/Even Effect in the Structure: XRD. In the previous sections, we have established a significant odd/even chain length alternation in T_m of stacked AgSC*n* lamella. The proposed phenomenological model showed that this variation is due to the difference in the excess interfacial energies between odd and even chains. We present a structural difference between odd and even AgSC*n* from the measurement of layer thickness obtained from XRD of multilayer AgSC*n* crystals.

Figure 12a shows the lamellar thickness as a function of the number of carbons in the alkyl chain without including the terminal CH_3 group ($n - 1$ carbons). When the data are separated between odd and even chains, there is a small but well-resolved variation in the thickness. The linear fit of the data for odd and even points shows two lines with the same slope but different offsets. The value of the slope corresponds to the increase in the thickness due to addition of two methyl groups (C−C−C distance). This value is known for polyethylene and alkane, which has alkyl chains that are not tilted (2.55 Å). For AgSC*n*, both odd and even alkyl chains are tilted 18 ± 1° relative to the central plane. This is the first time that the odd and even thicknesses are analyzed separately for AgSC*n*. We often find in the literature[28,30] that in typical XRD analysis there is no distinction between odd and even chains, which can yield conflicting values for tilt = 12 ± 3° with large experimental uncertainties.

The *y*-offsets of the linear fit include the thickness of the central plane and the terminal methyl groups at the interface. The central plane thickness does not change between odd and even AgSC*n*. The difference in the offsets is therefore attributed only to the difference in the interlayer packing between odd and even chains. This difference is 0.35 Å and is well-resolved as shown in the plots of the absolute deviation from the linear fit for each data points in Figure 12b. This odd/even difference

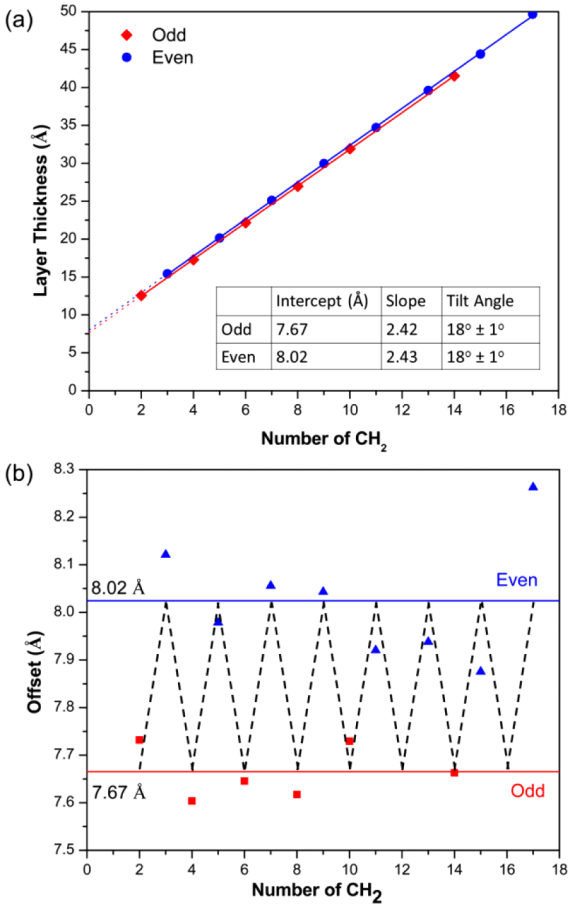

Figure 12. (a) Plot of lamella thickness vs number of CH_2 in the chains. Separate analyses of the odd and even chains show the same tilt angle but different *y*-offsets. (b) Plot of the deviation of the data from the linear fit which shows that the difference between the odd and even offsets is well-resolved.

in the thickness has been previously reported for alkanes using both molecular modeling of the structure and thickness measurements from XRD.[61] Structural models initially proposed by Kitaigorodsky and later developed from diffraction studies show a difference of 0.3 Å in the packing between odd and even alkanes.[57]

It is difficult to measure the thickness of a purely single-layer AgSC*n*. Previous X-ray reflectivity data are limited due to the difficulty in simulating the structure of the bilayer, while AFM step height measurements suffer from uncertainties in the substrate offsets.[36] However, we can calculate the differences between odd and even chains for the single layer by using the calculated tilt angle of the chain and the geometry of the bonding in the alkyl chains. This simple calculation shows an odd/even variation in the thickness with a difference of ~0.6 Å.

The offsets in AgSC*n* indicate that the odd chains have a lower van der Waal's gap, and thus the terminal methyl groups are closer at the interface. This closer interaction may account for the lower excess interfacial energy for the odd chains and a higher T_m compared to the even chains. In comparing AgSC*n* with alkanes with regard to the odd/even effect, we note both the similarities and contrasts of the two systems. The similarity is that the crystals with closer layer spacing (XRD) always have a higher T_m. The contrast is that closer layer spacing occurs for odd-chain in AgSC*n* but for even-chain in alkanes.[56] Therefore, it is not the feature/attribute of being either odd or even that

dx.doi.org/10.1021/ja4059958 | J. Am. Chem. Soc. 2013, 135, 14286−14298

directly controls the change in T_m but rather the nature of the interface, which is better characterized by layer spacing. We suggest that it is the combination of both the odd/even attribute and the tilt angle that together directly controls the nature of the interface and thus the value of T_m. These results can be generalized to other aliphatic lamellar systems that exhibit this odd/even effect.

4. CONCLUSION

We have done a systematic study of the melting of lamellar crystals of AgSC*n* using nanocalorimetry coupled with a new synthesis method. This method allows for precise control of the number of layers in the lamella. Discrete changes in the lamella thickness are achieved in two ways: change in chain length and change in the number of layers. Size-effect melting behavior is observed both as a function of chain length and number of layers.

For 1-layer AgSC*n*, magic size-effect melting behavior is observed. The change in chain length leads to the addition of a "shell" to the lamella analogous to the discrete addition of atomic shells in magic size metal clusters.

Stacking has a significant effect on the melting of AgSC*n*. There is a large increase in T_m between 1- and 2-layer samples. We have also shown a large odd/even effect for 2, 3, and 4 layers. This is unambiguously a result of stacking since no odd/even effect is observed for unstacked single-layer samples.

We developed a phenomenological model that explains the size-dependent melting in terms of the excess free energy contributions from the surface region, the interlayer interface, the substrate interface, and the central plane. The odd/even effect on 2, 3, and 4 layers can be explained by a significant difference between the interfacial energies of the odd and even chains. The model shows an increased stabilization of the interface for odd chains. This stabilization systematically decreases as the layer number is increased, which explains why no odd/even effect is observed for multilayer samples.

There is also an odd/even variation in the thickness of AgSC*n* lamella from XRD measurements, which is consistent with the deduced difference in the interface structure formed between odd and even chains, as is also the situation in the odd/even effect for alkanes.

■ ASSOCIATED CONTENT

Supporting Information

Detailed derivation and fitting procedure for the phenomenological model. This material is available free of charge via the Internet at http://pubs.acs.org.

■ AUTHOR INFORMATION

Corresponding Author

l-allen9@illinois.edu

Present Address

[§]Intel Corporation, Chandler, Arizona 85226, United States.

Author Contributions

Authors Lito P. de la Rama and Liang Hu contributed equally and share first author status.

Notes

The authors declare no competing financial interest.

■ ACKNOWLEDGMENTS

This work is supported by NSF-DMR-1006385. Materials characterization was carried out in part in the Frederick Seitz Materials Research Laboratory, University of Illinois. The nanocalorimetry sensors were fabricated at the Cornell Nanoscale Facility, a member of the National Nanotechnology Infrastructure Network (NNIN). M.E. is supported by NSF through the Nanoscale Science and Engineering Center at the University of Wisconsin (DMR-0832760). The authors thank Professor P. Braun, Professor J.-M. Zuo, and Professor J. Lyding for discussion. We also acknowledge James W. Mayer (1930−2013) for his contributions and insight in the art of characterizing thin films, especially for Rutherford Backscattering Technique (RBS).

■ REFERENCES

(1) Takagi, M. *J. Phys. Soc. Jpn.* **1954**, *9*, 359.
(2) Coombes, C. J. *J. Phys. F* **1972**, *2*, 441−449.
(3) Buffat, P.; Borel, J. P. *Phys. Rev. A* **1976**, *13*, 2287−2298.
(4) Jackson, C. L.; McKenna, G. B. *J. Chem. Phys.* **1990**, *93*, 9002−9011.
(5) Naitabdi, A.; Ono, L. K.; Cuenya, B. R. *Appl. Phys. Lett.* **2006**, *89*, 043101−043103.
(6) Mostafa, S.; Behafarid, F.; Croy, J. R.; Ono, L. K.; Li, L.; Yang, J. C.; Frenkel, A. I.; Cuenya, B. R. *J. Am. Chem. Soc.* **2010**, *132*, 15714−15719.
(7) Gandhi, D. D.; Lane, M.; Zhou, Y.; Singh, A. P.; Nayak, S.; Tisch, U.; Eizenberg, M.; Ramanath, G. *Nature* **2007**, *447*, 299-U2.
(8) Kowarski, L. *Phys. Rev.* **1950**, *78*, 477−479.
(9) Bethe, H. A.; Bacher, R. F. *Rev. Mod. Phys.* **1936**, *8*, 82−229.
(10) Hoare, M. R.; Pal, P. *Adv. Phys.* **1975**, *24*, 645−678.
(11) Knight, W. D.; Clemenger, K.; Deheer, W. A.; Saunders, W. A.; Chou, M. Y.; Cohen, M. L. *Phys. Rev. Lett.* **1984**, *52*, 2141−2143.
(12) Noya, E. G.; Doye, J. P. K.; Wales, D. J.; Aguado, A. *Eur. Phys. J. D* **2007**, *43*, 57−60.
(13) Echt, O.; Sattler, K.; Recknagel, E. *Phys. Rev. Lett.* **1981**, *47*, 1121−1124.
(14) Stephens, P. W.; King, J. G. *Phys. Rev. Lett.* **1983**, *51*, 1538−1541.
(15) Efremov, M. Y.; Schiettekatte, F.; Zhang, M.; Olson, E. A.; Kwan, A. T.; Berry, R. S.; Allen, L. H. *Phys. Rev. Lett.* **2000**, *85*, 3560−3563.
(16) Jadzinsky, P. D.; Calero, G.; Ackerson, C. J.; Bushnell, D. A.; Kornberg, R. D. *Science* **2007**, *318*, 430−433.
(17) Lai, S. L.; Guo, J. Y.; Petrova, V.; Ramanath, G.; Allen, L. H. *Phys. Rev. Lett.* **1996**, *77*, 99−102.
(18) Olson, E. A.; Efremov, M. Y.; Zhang, M.; Zhang, Z.; Allen, L. H. *J. Appl. Phys.* **2005**, *97*, 034304.
(19) Efremov, M. Y.; Olson, E. A.; Zhang, M.; Schiettekatte, F.; Zhang, Z. S.; Allen, L. H. *Rev. Sci. Instrum.* **2004**, *75*, 179.
(20) Lai, S. L.; Ramanath, G.; Allen, L. H.; Infante, P.; Ma, Z. *Appl. Phys. Lett.* **1995**, *67*, 1229−1231.
(21) Olson, E. A.; Efremov, M. Y.; Zhang, M.; Zhang, Z. S.; Allen, L. H. *J. Microelectromech. Syst.* **2003**, *12*, 355−364.
(22) Denlinger, D. W.; Abarra, E. N.; Allen, K.; Rooney, P. W.; Messer, M. T.; Watson, S. K.; Hellman, F. *Rev. Sci. Instrum.* **1994**, *65*, 946−959.
(23) Zhang, M.; Efremov, M. Y.; Schiettekatte, F.; Olson, E. A.; Kwan, A. T.; Lai, S. L.; Wisleder, T.; Greene, J. E.; Allen, L. H. *Phys. Rev. B* **2000**, *62*, 10548−10557.
(24) Olson, E. A.; Efremov, M. Y.; Zhang, M.; Zhang, Z. S.; Allen, L. H. *J. Appl. Phys.* **2005**, *97*, 034304.
(25) Efremov, M. Y.; Olson, E. A.; Zhang, M.; Zhang, Z.; Allen, L. H. *Phys. Rev. Lett.* **2003**, *91*, 85703.
(26) Zhang, Z. S.; Wilson, O. M.; Efremov, M. Y.; Olson, E. A.; Braun, P. V.; Senaratne, W.; Ober, C. K.; Zhang, M.; Allen, L. H. *Appl. Phys. Lett.* **2004**, *84*, 5198.
(27) Hu, L.; Zhang, Z. S.; Zhang, M.; Efremov, M. Y.; Olson, E. A.; de la Rama, L. P.; Kummamuru, R. K.; Allen, L. H. *Langmuir* **2009**, *25*, 9585−9595.

(28) Dance, I. G.; Fisher, K. J.; Banda, R. M. H.; Scudder, M. L. *Inorg. Chem.* **1991**, *30*, 183−187.
(29) Fijolek, H. G.; Grohal, J. R.; Sample, J. L.; Natan, M. J. *Inorg. Chem.* **1997**, *36*, 622−628.
(30) Bensebaa, F.; Ellis, T. H.; Kruus, E.; Voicu, R.; Zhou, Y. *Langmuir* **1998**, *14*, 6579−6587.
(31) Baena, M. J.; Espinet, P.; Lequerica, M. C.; Levelut, A. M. *J. Am. Chem. Soc.* **1992**, *114*, 4182−4185.
(32) Levchenko, A. A.; Yee, C. K.; Parikh, A. N.; Navrotsky, A. *Chem. Mater.* **2005**, *17*, 5428−5438.
(33) Voicu, R.; Badia, A.; Morin, F.; Lennox, R. B.; Ellis, T. H. *Chem. Mater.* **2000**, *12*, 2646−2652.
(34) Popoff, R. T. W.; Zavareh, A. A.; Kavanagh, K. L.; Yu, H.-Z. *J. Phys. Chem. C* **2012**, *116*, 17040−17047.
(35) Radha, B.; Liu, G.; Eichelsdoerfer, D. J.; Kulkarni, G. U.; Mirkin, C. A. *ACS Nano* **2013**, *7*, 2602−2609.
(36) Hu, L.; de la Rama, L. P.; Efremov, M. Y.; Anahory, Y.; Schiettekatte, F.; Allen, L. H. *J. Am. Chem. Soc.* **2011**, *133*, 4367−4376.
(37) Kummamuru, R. K.; Hu, L.; Cook, L.; Efremov, M. Y.; Olson, E. A.; Allen, L. H. *J. Micromech. Microeng.* **2008**, *18*, 095027.
(38) Lai, S. L.; Ramanath, A. G.; Allen, L. H.; Infante, P. *Appl. Phys. Lett.* **1997**, *70*, 43−45.
(39) Thomson, J. J. *Application of Dynamics to Physics and Chemistry*; McMillan: London, 1888.
(40) Pawlow, P. *Z. Phys. Chem.* **1909**, *65*, 545.
(41) Hoffman, J.; Weeks, J. *J. Chem. Phys.* **1965**, *42*, 4301−4302.
(42) Wunderlich, B.; Czornyj, G. *Macromolecules* **1977**, *10*, 906−913.
(43) Lauritzen, J.; Hoffman, J. *J. Chem. Phys.* **1959**, *31*, 1680.
(44) Lauritzen, J.; Hoffman, J. *J. Res. Natl. Bur. Stand., Sect. A* **1960**, *64*, 73−102.
(45) Hoffman, J.; Weeks, J. *J. Res. Natl. Bur. Stand., Sect A* **1962**, *66A*, 16−28.
(46) Ulman, A. *Chem. Rev.* **1996**, *96*, 1533−1554.
(47) Ulman, A. *Self-Assembled Monolayers of Thiols*; Academic Press: San Diego, CA, 1998; Vol. *24*.
(48) Love, J. C.; Estroff, L. A.; Kriebel, J. K.; Nuzzo, R. G.; Whitesides, G. M. *Chem. Rev.* **2005**, *105*, 1103−1169.
(49) Fenter, P.; Eisenberger, P.; Liang, K. S. *Phys. Rev. Lett.* **1993**, *70*, 2447−2450.
(50) Ramin, L.; Jabbarzadeh, A. *Langmuir* **2011**, *27*, 9748−9759.
(51) Srivastava, P.; Chapman, W. G.; Laibinis, P. E. *Langmuir* **2005**, *21*, 12171−12178.
(52) Tao, F.; Bernasek, S. L. *Chem. Rev.* **2007**, *107*, 1408−1453.
(53) Small, D. M. *The Physical Chemisty of Lipids from Alkanes to Phospholipids*; Plenum Press: New York, 1986.
(54) McGonigal, G. C.; Bernhardt, R. H.; Thomson, D. J. *Appl. Phys. Lett.* **1990**, *57*, 28−30.
(55) Rabe, J. P.; Buchholz, S. *Science* **1991**, *253*, 424−427.
(56) Boese, R.; Weiss, H.-C.; Blaser, D. *Angew. Chem., Int. Ed.* **1999**, *38*, 988−992.
(57) Kitaigorodskii, A. I. *Organic Chemical Crystallography*; Consultants Bureau: New York, 1961.
(58) Kwan, A. T.; Efremov, M.; Olson, E. A.; Schiettekatte, F.; Zhang, M.; Geil, P. H.; Allen, L. H. *J. Polym. Sci., Part B: Polym. Phys.* **2001**, *39*, 1237−1245.
(59) Wunderlich, B. *Thermal Analysis of Polymeric Materials*; Springer-Verlag: Berlin, 2005.
(60) Hohne, G. W. H. *Polymer* **2002**, *43*, 4689−4698.
(61) Dorset, D. L. *Crystallography of the Polymethylene Chain*; Oxford University Press: New York, 2005.